Mammalian Biology
https://doi.org/10.1007/s42991-021-00174-7

METHODOLOGY

Automated, high-throughput image calibration for parallel-laser photogrammetry

Jack L. Richardson[1] · Emily J. Levy[2] · Riddhi Ranjithkumar[3] · Huichun Yang[4,5] · Eric Monson[6] · Arthur Cronin[7,8] · Jordi Galbany[1,9] · Martha M. Robbins[10] · Susan C. Alberts[2,11] · Mark E. Reeves[7] · Shannon C. McFarlin[1]

Received: 15 January 2021 / Accepted: 21 August 2021

Abstract

Parallel-laser photogrammetry is growing in popularity as a way to collect non-invasive body size data from wild mammals. Despite its many appeals, this method requires researchers to hand-measure (i) the pixel distance between the parallel laser spots (inter-laser distance) to produce a scale within the image, and (ii) the pixel distance between the study subject's body landmarks (inter-landmark distance). This manual effort is time-consuming and introduces human error: a researcher measuring the same image twice will rarely return the same values both times (resulting in within-observer error), as is also the case when two researchers measure the same image (resulting in between-observer error). Here, we present two independent methods that automate the inter-laser distance measurement of parallel-laser photogrammetry images. One method uses machine learning and image processing techniques in Python, and the other uses image processing techniques in *ImageJ*. Both of these methods reduce labor and increase precision without sacrificing accuracy. We first introduce the workflow of the two methods. Then, using two parallel-laser datasets of wild mountain gorilla and wild savannah baboon images, we validate the precision of these two automated methods relative to manual measurements and to each other. We also estimate the reduction of variation in final body size estimates in centimeters when adopting these automated methods, as these methods have no human error. Finally, we highlight the strengths of each method, suggest best practices for adopting either of them, and propose future directions for the automation of parallel-laser photogrammetry data.

Keywords Automation · Baboon · Gorilla · Image processing · Machine learning · Parallel-laser photogrammetry

Handling editors: Leszek Karczmarski and Scott Y.S. Chui.

Jack L. Richardson and Emily J. Levy are co-first authors and contributed equally.

This article is a contribution to the special issue on "Individual Identification and Photographic Techniques in Mammalian Ecological and Behavioural Research – Part 1: Methods and Concepts" — Editors: Leszek Karczmarski, Stephen C. Y. Chan, Daniel I. Rubenstein, Scott Y.S. Chui and Elissa Z. Cameron.

✉ Shannon C. McFarlin
scmcfarlin@gmail.com

[1] Department of Anthropology, Center for the Advanced Study of Human Paleobiology, The George Washington University, Science and Engineering Hall, 800 22nd St. NW, Suite 6000, Washington, DC 20052, USA

[2] Department of Biology, Duke University, 130 Science Drive, Durham, NC 27708, USA

[3] Pratt School of Engineering, Duke University, 305 Teer Engineering Building, Durham, NC 27708, USA

[4] Department of Computer Science, The George Washington University, Science and Engineering Hall, 800 22nd St. NW, Room 4000, Washington, DC 20052, USA

[5] Amazon Web Services, Identity Service, 410 Terry Ave N, Seattle, WA 98019, USA

[6] Duke University Libraries, Duke University, 226 Bostock Library, Box 104732, Durham, NC 27708, USA

[7] Department of Physics, The George Washington University, 725 21st St NW, Washington, DC 20052, USA

[8] Applied Materials, 3050 Bowers Avenue, Santa Clara, CA 95054, USA

[9] Department of Clinical Psychology and Psychobiology, University of Barcelona, Campus Mundet, Pg. de la Vall d'Hebron 171, 08035 Barcelona, Spain

[10] Max Planck Institute for Evolutionary Anthropology, Deutscher Platz 6, 04013 Leipzig, Germany

[11] Department of Evolutionary Anthropology, Duke University, 130 Science Drive, Durham, NC 27708, USA

Published online: 11 March 2022

Introduction

Body size measurements of wild animals are frequently used to study effects of social, environmental, and anthropogenic factors on growth and health (e.g., Altmann and Alberts 2005; Swenson et al. 2007; Gardner et al. 2011; Berger 2012; Lourie et al. 2014; Tarugara et al. 2019). One common non-invasive method to collect these data is parallel-laser photogrammetry. This method involves projecting parallel lasers of known physical distance (inter-beam distance) onto the study animal, thereby creating a scale when the animal is photographed (Fig. 1). Parallel-laser photogrammetry is a reliable and efficient method to determine the body size of living wild animals, whose measurement would otherwise require capture or anesthetization. In contrast to other photogrammetry techniques, parallel-laser photogrammetry does not require information on the distance between the camera and the study subject, a requirement that slows data collection and can be challenging to obtain and record. Parallel-laser photogrammetry was first used to measure body sizes of killer whales (*Orcinus orca*, Durban and Parsons 2006) and Alpine ibex (*Capra ibex*, Bergeron 2007). The method has since become more widely-used across taxa, particularly among large animals such as whales (Webster et al. 2010; Durban et al. 2017; Wong and Auger-Méthé 2018), cartilaginous fishes (Deakos 2010; Rohner et al. 2011; Jeffreys et al. 2013), horses (Weisgerber et al. 2015), elephants (Wijeyamohan et al. 2012), and primates (Rothman et al. 2008; Barrickman et al. 2015; Lu et al. 2016; Galbany et al. 2017; Wright et al. 2019, 2020).

Despite its utility, parallel-laser photogrammetry requires substantial manual effort to measure images on the computer. For each collected image, the position of each laser spot on the image must be measured to produce an inter-laser distance in pixels (Fig. 1). By dividing the inter-beam distance (i.e. the physical distance between the laser beams) in centimeters by the inter-laser distance, a scale is calculated for the image in centimeters per pixel. The researcher must also locate and measure the distance between the landmarks on the body in pixels (inter-landmark distance). The inter-landmark distance is multiplied by the scale to produce a body size estimate in centimeters (Fig. 1). Some researchers take each measurement twice, which doubles measurement time (e.g., Lu et al. 2016). To our knowledge, only one software package, AragoJ, is designed to reduce the burden of parallel-laser photogrammetry (Aleixo et al. 2020). AragoJ streamlines the processing pipeline because it allows researchers to calculate the image scale, manually measure images, access image metadata, and perform data organizing and cleaning within a single software package. However, the manual effort of measuring inter-laser distances remains a barrier to increasing the throughput of image measurements.

In addition to a more high-throughput workflow, greater automation of the measurement process also would increase precision of the final estimates of body size produced using parallel-laser photogrammetry. While researchers must grapple with multiple sources of measurement uncertainty in parallel-laser photogrammetry methods (e.g. parallax, pixel density, apparatus properties, picture quality, lens distortion, improper alignment; see Durban and Parsons 2006; Bergeron 2007; Galbany et al. 2016), one unavoidable source of measurement uncertainty is human error. One observer measuring the same image twice will produce two different values (resulting in within-observer error), as will two observers measuring the same image (resulting in between-observer error). Two techniques to automate this

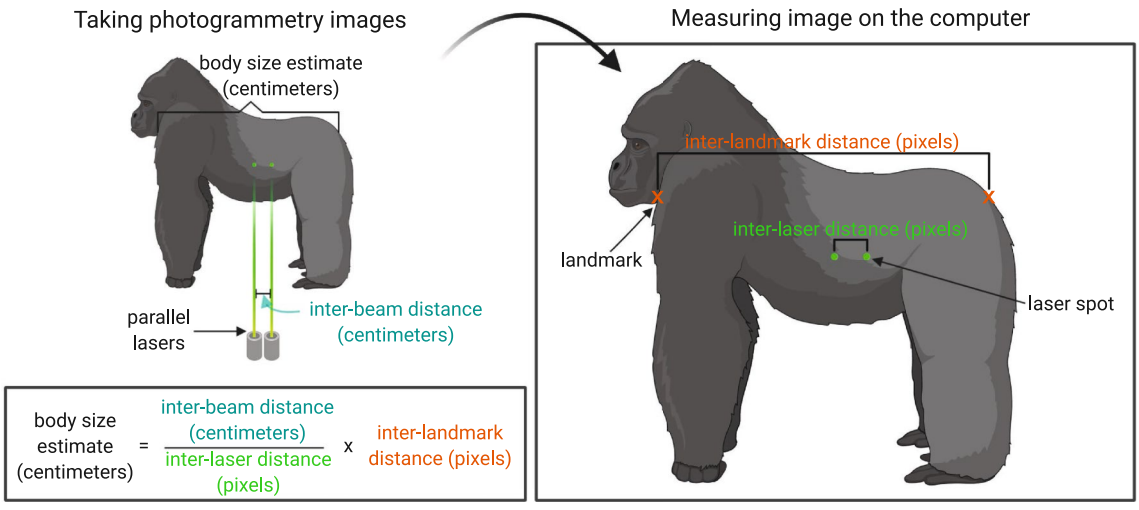

Fig. 1 Terminology and calculations for estimating body size of study animal using parallel-laser photogrammetry. Note that the image datasets used to validate the *ImageJ* and *skimage* methods have three laser spots. Created with BioRender.com

process are image processing and machine learning. Image processing methods allow detailed analysis of image characteristics, such as color, brightness, object shape, and object size. These analytical tools have become highly accessible with the development of user-friendly interfaces such as ImageJ (Schneider et al. 2012), but are often more customizable in coding platforms such as the Scikit-image (i.e., skimage) Python package (van der Walt et al. 2014). Machine learning can also automate laborious image-analysis tasks and may identify new patterns not detected by humans (e.g., Clapham et al. 2020; Vaid et al. 2020). Given the customizability and power of image processing and machine learning, these technologies are useful tools to apply to parallel-laser photogrammetry analyses.

Here we present and compare two different methods (*skimage* and *ImageJ*) to automate the process of measuring the inter-laser distance in a parallel-laser photogrammetry image. Below, we describe the two automated methods and assess their precision and whether they introduce systematic error. We then compare their performance on novel datasets, test whether they reduce human error, and discuss their applicability to new projects. We show that both methods reduce manual effort and return measurements equivalent to manual image measurements and to each other, indicating high precision without sacrificing accuracy.

Workflow for the *skimage* and *ImageJ* methods

The *skimage* approach was developed at The George Washington University to measure images taken for a longitudinal study of mountain gorillas (*Gorilla beringei beringei*) in Bwindi Impenetrable National Park, Uganda (2015–present, the Bwindi Gorilla Project, managed by Max Planck Institute for Evolutionary Anthropology). The *ImageJ* method was created at Duke University to measure images taken of savannah baboons (*Papio cynocephalus*) in Amboseli National Park, Kenya during a short-term field study (2017–2019).

The *skimage* method is a hybrid method that uses machine learning to first identify and isolate pixel areas (or 'masks') that contain primate subjects within photographs, and then processes these masks using the scikit-image (hereafter *skimage*) package in Python (van der Walt et al. 2014) to identify green laser spots based on RGB ratios, color intensity, size and circularity (Fig. 2). The *skimage* method requires familiarity with coding in Python and high computing power to implement machine learning (though it can be used without machine learning pre-processing; see Appendix: Table A1), but once implemented it runs with minimal intervention. The *ImageJ* method uses the image processing software ImageJ (Schneider et al 2012) to crop photos and identify green laser spots based on color and brightness (Fig. 3). The *ImageJ* method is easily implemented without specific programming knowledge but requires the researcher to manually crop approximately 50% of the images.

Validating methods

Assessing *skimage* and *ImageJ* methods' success rate

The *skimage* method successfully identified the laser spots in 99.0% (100/101) of gorilla images. The *skimage* method's computing time is approximately 2 min per image (Appendix: Table A2). The *ImageJ* method successfully identified the laser spots in 91.4% (1937/2119) of baboon images. It's computing time is approximately 2–3 s per image, with an additional 5 s per image of manual effort if the image is manually cropped (Appendix: Table A2). The validation datasets used below are comprised of 100 images of each species in which the laser spots were successfully identified.

Comparing *skimage* and *ImageJ* methods to manual image measurements

To assess precision in inter-laser distance measurement, we compared measurements generated using each automated method to measurements collected manually. For the *skimage* validation we used a dataset of 100 gorilla images; 74 images were in lateral view and 26 images were in dorsal view. The dataset included images of gorillas of both sexes (64 male and 36 female) and all age classes (15 infants [0–3.5 years], 11 juveniles [3.5–6 years], 12 sub-adults [6–8 years], 10 blackbacks [males 8–12 yrs], 16 adult females [> 8 years] and 35 silverbacks [males > 12 years]). Images were taken using a Nikon D800 DSLR camera (36.3 megapixel, 4.88 µ pixel size) with an AF-S Nikkor 85 mm f/1.4G lens or a Canon EOS 5D Mark III DSLR (22.3 megapixel, 6.25 µ pixel size) with a Canon EF 17–35 mm f/2.8L USM lens. All manual measurements were collected by the same author (JLR). For the *ImageJ* validation we used a dataset of 100 successful baboon images; all images were in lateral view. The dataset included images of baboons of both sexes (71 females, 29 males) and all age classes (13 infants and juveniles [0–2.5 years], 8 subadult males [5–7 years], 10 adult males [> 7 years], and 69 adult females [> 4 years]). Images were taken using an Olympus OM-D EM-5 Mark II mirrorless camera (15.9 megapixel, 3.75 µ pixel size) with an M. Zuiko 12–100 mm f/4 IS Pro Digital lens. All manual measurements were collected by the same observers (lasers: E. Malone; body landmarks: EJL). All images were taken from a distance of approximately 5–15 m from the study subjects (gorillas, 7–12 m; baboons 5–15 m) in line with other parallel-laser photogrammetry studies (e.g.,

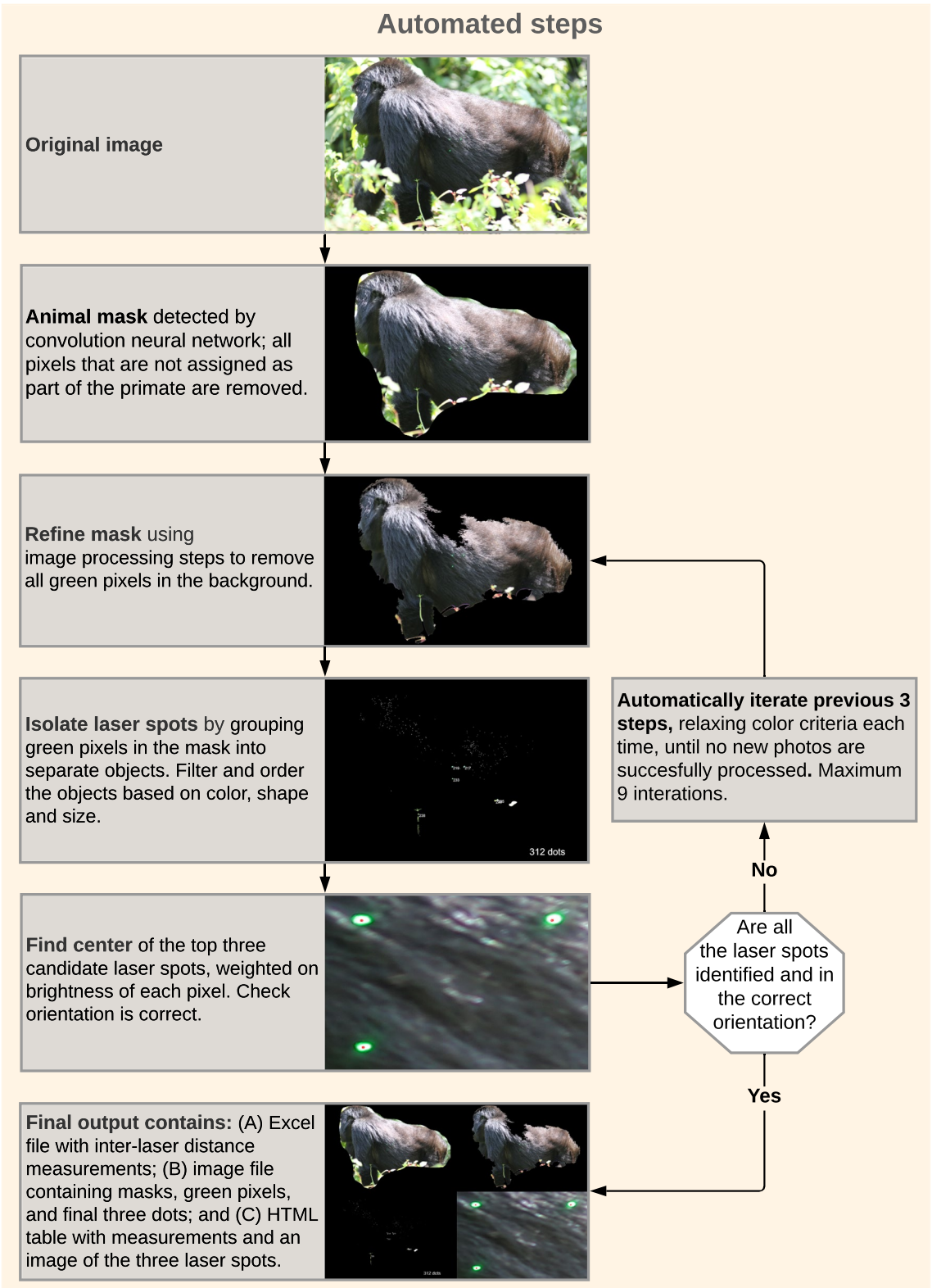

Fig. 2 Flowchart of automated steps used to process images using the *skimage* method. After running the script, manual adjustments can be made to some parameters to improve performance on unsuccessful images. For the annotated script, see Supplement. Any images that are not successful after these adjustments must be hand-measured. Created with Lucidchart

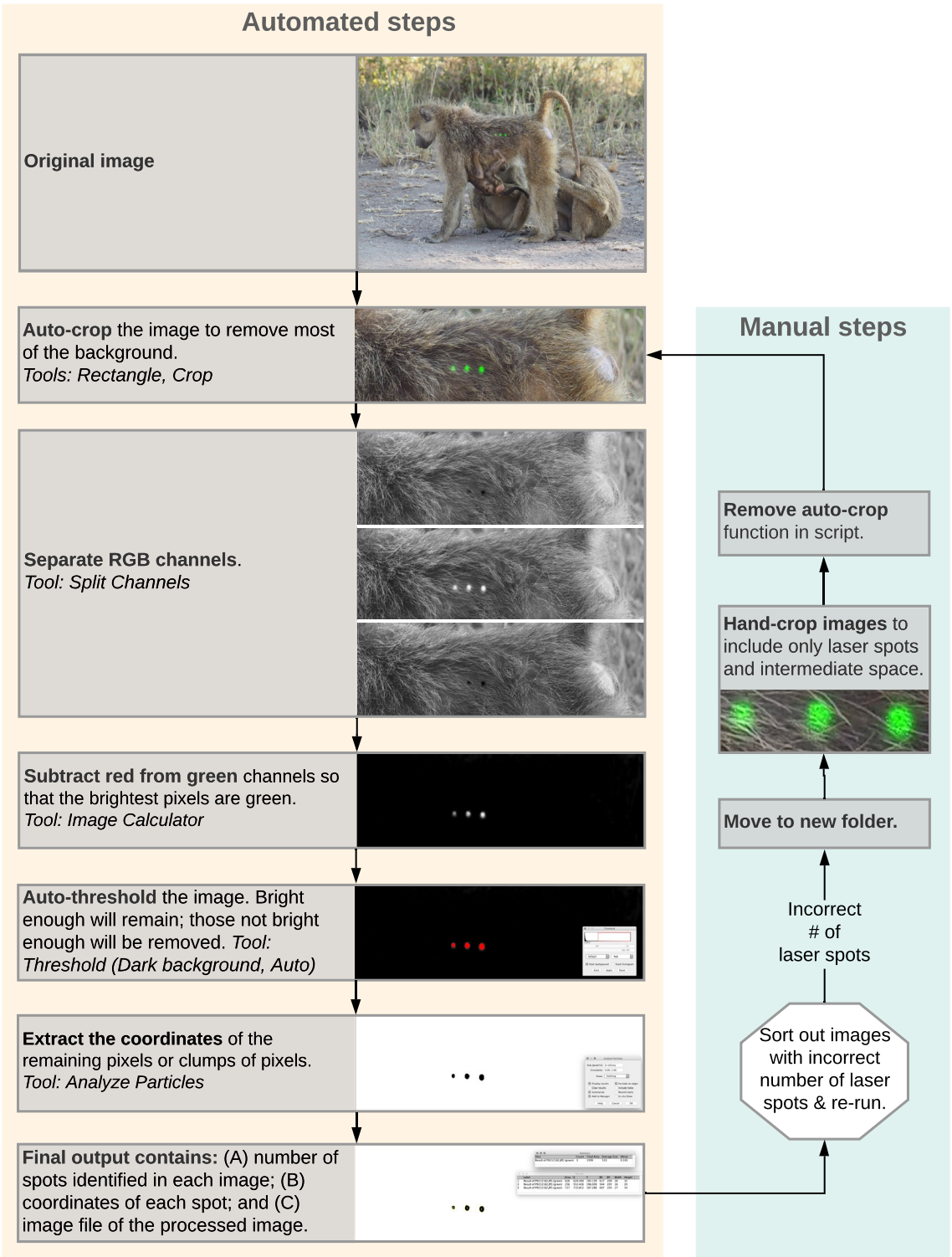

Fig. 3 Flowchart of automated and manual steps used to process images using the *ImageJ* method. For the annotated script, see Supplement. Any images that are not successful after reprocessing must be hand-measured. Created with Lucidchart

Rothman et al. 2008; Galbany et al. 2016). These distances between camera and subject are within the technical and practical range for using parallel-laser photogrammetry.

The laser spot orientations of the gorilla and baboon image datasets were different: the gorilla images had three laser spots in a triangular orientation (Fig. 2), and the

baboon images had two or three in a horizontal line (Fig. 3). For our analysis of the gorilla images, we only used the horizontal inter-beam distance, which was 2 cm (19 images), 4 cm (76 images), or 4.5 cm (5 images). For baboon images, inter-beam distance was 2 cm for images with two laser spots (8 images) or 4 cm for images with three laser spots (92 images; the maximum inter-beam distance). Both methods can be adjusted to measure datasets with more or fewer than three laser spots, as well as datasets where the laser spots are in different orientations (see Supplement).

For each image, we compared either the *skimage* method (in the case of gorilla photos) or the *ImageJ* method (in the case of baboon photos) to the manual method by calculating the pixel difference and percent difference. The pixel difference was calculated by subtracting the automated method's inter-laser distance from the manual method's inter-laser distance. The percent difference was calculated by dividing the pixel difference by the manual inter-laser distance and multiplying by 100; thus, the percent difference represents the pixel difference as a percent of the manually-measured inter-laser distance. When comparing automated methods to each other, pixel difference was calculated by subtracting *ImageJ* from *skimage,* and percent difference was calculated by dividing the pixel difference by the mean of the two automated measures. The percent difference controls for the fact that images were taken at different resolutions and distances, resulting in different centimeter-to-pixel conversions for each image. The pixel difference is not affected by

Table 1 Percent differences [and pixel differences] among inter-laser distances measured manually vs. the *ImageJ* method, manually vs. the *skimage* method and via the *ImageJ* method vs. the *skimage* method on both study animal datasets; diff = difference

	Species	Comparison	Mean % diff [pixel diff]	SD of % diff [pixel diff]	Range of % diff [pixel diff]
1	**Gorilla**	**Skimage vs. manual**	**– 0.004 [0.004]**	**0.710 [0.913]**	**– 1.58, 4.34 [– 2.88, 3.33]**
2	Gorilla	ImageJ vs. manual	0.075 [0.193]	1.180 [1.98]	– 4.92, 5.56 [– 5.39, 10.6]
3	Gorilla	Skimage vs. imageJ	0.089 [0.208]	0.998 [1.67]	– 3.33, 5.53 [– 3.77, 10.2]
4	**Baboon**	**ImageJ vs. manual**	**0.008 [– 0.041]**	**0.903 [0.784]**	**– 3.98, 4.94 [– 3.18, 2.15]**
5	Baboon	Skimage vs. manual	– 0.063 [– 0.064]	0.904 [0.929]	– 3.64, 3.28 [– 3.12, 2.08]
6	Baboon	ImageJ vs. skimage	0.050 [– 0.006]	0.897 [0.671]	– 2.43, 6.36 [– 2.26, 2.72]

Bolded rows represent comparisons of the manual method with the automated method that was originally created for that species (*skimage* for gorillas, *ImageJ* for baboons)

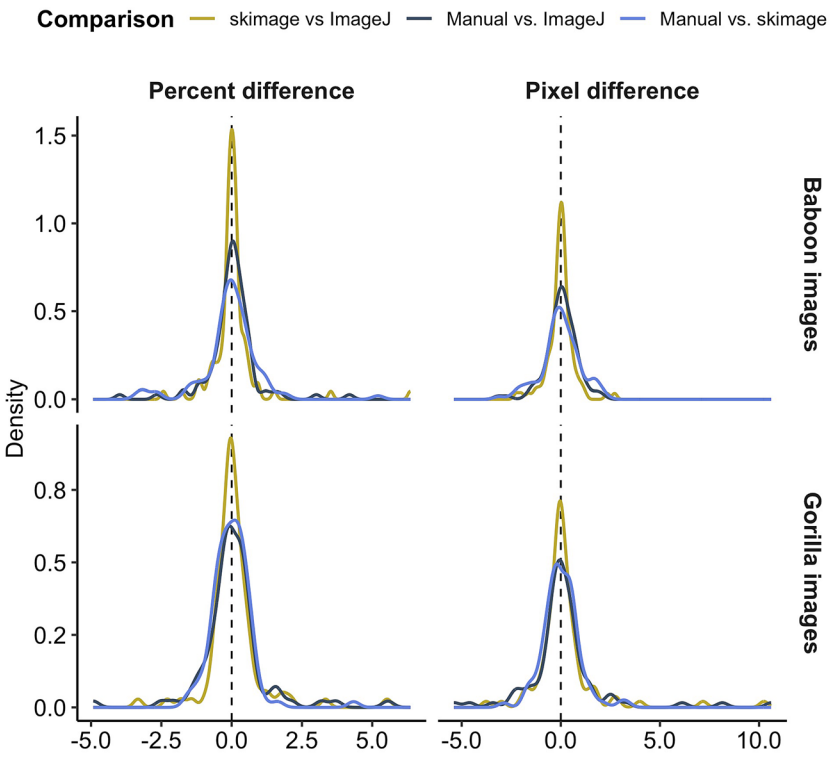

Fig. 4 Distribution of percent differences (left column) and pixel differences (right column) when comparing inter-laser distances measured manually vs. using the *skimage* method (light blue lines), manually vs. using the *ImageJ* method (dark blue lines) and using the *skimage* method vs. using the *ImageJ* method (yellow lines) for images of baboons (top row) and gorillas (bottom row). Peaks close to zero indicate negligible systematic bias, and narrower peaks indicate higher precision

inter-beam distance (in centimeters), whereas for the same pixel difference, the percent difference will be higher when the inter-beam distance is smaller. The pixel difference and the percent difference are both measures of precision, i.e., of how close the automated measures of inter-laser distance are to the manual measures. We present our results here as the mean percent or pixel difference ± standard deviation (SD). Means close to zero indicate that the automated methods lack systematic bias. In combination with low SDs, means close to zero indicate high precision of the automated methods. Although we cannot directly test accuracy because the true inter-laser distance is unknown, convergence between methods would suggest high accuracy. For the absolute values of the means and SDs, see Appendix Table A3.

Both the *skimage* and *ImageJ* automated methods produced inter-laser distances that were highly consistent with the manual measures, indicating high precision and no evidence of systematic bias. For the *skimage* method applied to the gorilla images, the mean percent difference between the automated and manual inter-laser distances was − 0.004% ± 0.710% and the mean pixel difference was 0.004 ± 0.913 pixels (Table 1 row 1; Fig. 4 bottom row, light blue lines). For the *ImageJ* method applied to the baboon images, the mean percent difference between the automated and manual inter-laser distances was 0.008% ± 0.903%, and the mean pixel difference was − 0.041 ± 0.784 pixels (Table 1 row 4; Fig. 4 top row, dark blue lines). When using the *ImageJ* method on the baboon images, 44/100 images had to be hand-cropped (Fig. 3).

Testing *skimage* and *ImageJ* methods with novel datasets

To test how adaptable our automated methods were to new datasets, we next used the *skimage* method to measure the validation images of baboons and the *ImageJ* method to measure the validation images of gorillas. Both methods required alterations to optimize performance on this new set of images.

Skimage method on baboon images

To adapt the *skimage* method to work on baboon images, we altered the orientation check (Fig. 2). The gorilla images have three laser spots oriented in a right-angle triangle and the baboon images have two or three laser spots oriented in a straight line. After changing the orientation check, the *skimage* method identified the correct number of laser spots in 98/100 baboon images. The method produced inter-laser distances highly consistent with manual image measurements (mean percent difference = − 0.063% ± 0.904%; mean pixel difference = − 0.064 ± 0.929 pixels; Table 1, row 5; Fig. 4 top row, light blue lines).

ImageJ method on gorilla images

The biggest challenge with this new set of images was that the *ImageJ* method relies on isolating green pixels, and the background of most gorilla images is predominantly green. A smaller automated crop (Fig. 3, *Auto-crop*) was able to circumvent this issue for only 17/100 images. The most success was achieved by hand-cropping all images to include only the three laser spots and intermediate space. Without any other changes to the *ImageJ* code, this method retrieved the correct number of laser spots for 88/100 images. As with the *skimage* comparison, these measurements were highly consistent with manual image inter-laser distances (mean percent difference = 0.075% ± 1.18%; mean pixel difference = 0.193 ± 1.98 pixels; Table 1, row 2; Fig. 4 bottom row, dark blue lines).

Skimage vs. *ImageJ*

Finally, we compared the inter-laser distances produced by the two automated methods to each other. The means and SDs of these two automated methods compared to each other were highly consistent with the means and SDs of each automated method relative to manual measures (Table 1, rows 3 & 6). However, the automated vs. automated comparison yielded more percent differences and pixel differences close to 0 than the automated vs. manual comparisons (Fig. 4, yellow lines compared to light and dark blue lines). We interpret this to mean that for most images, both automated methods are more precise and more accurately identify the central point of the laser spot than human observers.

Measuring uncertainty

Uncertainty (i.e., variation) in parallel-laser photogrammetry measurements is inherent, and automating some steps may reduce uncertainty. One source of uncertainty is human error: when we measure the inter-laser distance or the inter-landmark distance in pixels (Fig. 1) twice on the same image, we rarely record the exact same measurement both times. Variation in these measurements will affect the body size estimate in centimeters. Here, we calculate how much the uncertainty in the body size estimate is reduced when adopting an automated method. Our calculations reflect within-observer human error, but our findings can be extrapolated to between-observer human error (see "Discussion").

The effect of human error on the uncertainty of the body size estimate can be quantified using the Propagation of Uncertainty Equation. For terms that are multiplied and/or divided (see calculation in Fig. 1) the Propagation of Uncertainty Equation is:

$$U_{\text{body size estimate}} = \sqrt{U^2_{\text{inter-laser}} + U^2_{\text{inter-landmark}}}$$

where U is a measure of uncertainty such as standard deviation (de Forest Palmer 1912; Bevington and Robinson 2002). This equation informs us that both components—variation in the inter-laser distance and variation in the inter-landmark distance—equally affect the variation in our body size estimate. If the variation in one of these components is much larger than the other, it will be the main source of variation in the body size estimate.

To estimate how much variation in our body size estimate is due to within-observer human error, we first calculated two components of variance from 100 images of adult female baboons with inter-laser distances of 4 cm:

1. Variance in manual inter-laser distance (*inter-laser*): For each of the 100 images, the inter-laser distance was measured, in pixels, two times by the same observer (E. Malone). The difference between the two measurements was divided by the mean of the two measurements and multiplied by 100 to calculate a within-observer percent difference.
2. Variance in inter-landmark distance (*inter-landmark)*: Inter-landmark distance was measured, in pixels, for three different body size measures—shoulder-rump (n = 67 images), leg ($n = 71$), and forearm ($n = 68$)—these were measured two times for each image by the same author (EJL). We did not measure all three body size estimates in every image. The difference between the two measurements was divided by the mean of the two measurements and multiplied by 100 to calculate a within-observer percent difference.

Note that this is different from the percent difference calculated above; see "Validating methods". We then calculated the mean, standard deviation, and range of those within-observer percent differences (Table 2, Fig. 5). Finally, we used the standard deviations of those within-observer percent differences in the Equation for Uncertainty Propagation:

$$\text{SD}_{\text{body size estimate}} = \sqrt{\text{SD}^2_{\text{inter-laser}} + \text{SD}^2_{\text{inter-landmark}}}$$

This calculates a standard deviation of the final body size estimates of 1.07%, 1.06%, and 1.76% for baboon shoulder-rump, leg, and forearm lengths, respectively. This means that final body size estimates in centimeters will have standard deviations of 1–2% that are derived solely from within-observer human error in manually measuring inter-laser distances and inter-landmark distances.

The automated method generates inter-laser distances with no statistical uncertainty because it always returns the same inter-laser distance for a particular image. Therefore, the automated methods both produce $\text{SD}^2_{\text{inter-laser}} = 0$. The standard deviation in the shoulder-rump, leg, and forearm estimates in centimeters are reduced to 0.60%, 0.59%, and 1.52%, respectively. These values are equal to only the component of uncertainty associated with manually measuring inter-landmark distances. Note that the decrease in uncertainty is smaller for the forearm measurement than the shoulder-rump and leg measurements. This is because variance in the inter-landmark distance of the forearm was largest (due to it being a smaller measurement and/or having more difficult landmarks to pinpoint), so it consumed a larger proportion of the uncertainty relative to the shoulder-rump and leg variances.

In other words, using the automated inter-laser distance instead of the manual inter-laser distance approximately halves the uncertainty in the baboon shoulder-rump and leg estimates that is due to within-observer human error, thereby increasing the precision of these body size estimates. Because the automated and manual inter-laser distance measurements were highly consistent with each other (see "Validating methods"), our increases in precision do not sacrifice accuracy. Further, in studies in which multiple observers perform manual measurements (e.g., Galbany et al. 2016; Lu et al. 2016), an automated method would further reduce variation in the body size estimates that is due to between-observer human error.

Table 2 Sample size, mean, SD and range of within-observer differences, in pixels, for the two components of within-observer variance that were calculated to estimate propagated uncertainty; the manual body size variance was measured for three baboon body parts (shoulder-rump, leg, forearm)

Component of variance	# images	Mean within-observer % difference	SD of within-observer % difference	Range of within-observer % difference
Inter-laser	100	– 0.042	0.885	– 4.113, 2.578
Inter-landmark: shoulder-rump	67	0.016	0.595	– 1.345, 2.317
Inter-landmark: leg	71	– 0.022	0.585	– 2.793, 1.418
Inter-landmark: forearm	68	0.137	1.523	– 4.438, 4.238

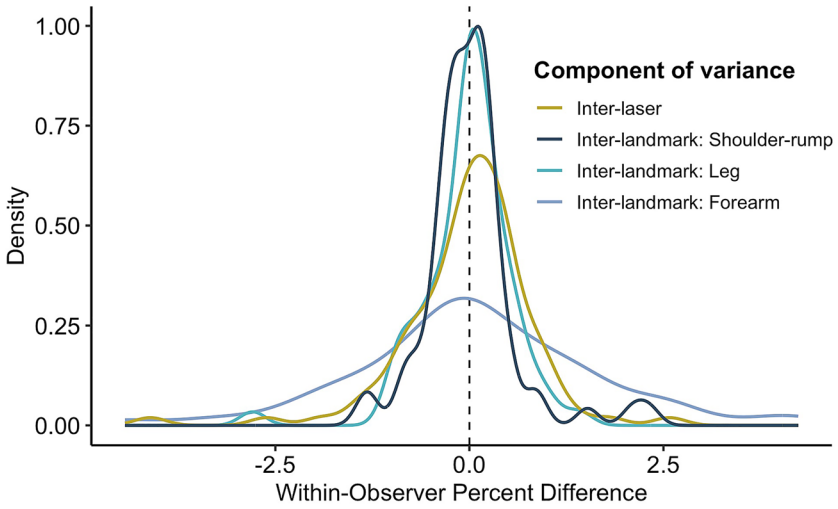

Fig. 5 Distributions of within-observer percent differences for the two components of variation (manual measures of inter-laser distance and inter-landmark distance) that we calculated to estimate uncertainty propagation from human error in baboon images. Removing variation in inter-laser distance using the automated methods approximately halves the variation in the body size estimate that is due to within-observer human error (see "Measuring uncertainty"). Because the automated method produces very similar measurements to the manual method (see "Validating methods"), substituting the automated for the manual method increases precision without sacrificing accuracy

Discussion

Summary of results

The manual effort needed to collect and process parallel-laser photogrammetry images is a barrier to its uptake. The two automated methods presented here save time and increase precision without compromising the accuracy of the measurements. The automated methods allow high-throughput image calibration, with little to no manual intervention. They yield inter-laser distances that are nearly identical to manual measurements on two datasets, indicating a lack of systematic error and high precision (Table 1, Fig. 4). Measurements from the two automated methods were highly consistent with each other, suggesting they are more accurate in their identification of the central point of the laser spot than human observers. Automated methods provide a more efficient way to increase accuracy compared to repeated manual measures. Finally, the automated methods increase measurement precision because they effectively remove uncertainty due to human error introduced while manually measuring the inter-laser distance.

Extending uncertainty estimates

Switching to an automated laser measurement reduced uncertainty in the final body size measurement due to within-observer error by approximately 0.5% SD. Within-observer error (typically calculated as % coefficient of variation [CV], which is comparable in magnitude to our within-observer percent difference measure) ranges from 0.5 to 2% in many previous studies (Breuer et al. 2007; Galbany et al. 2016; Lu et al. 2016; Wright et al. 2019). Additionally, automated methods will reduce uncertainty due to between-observer error which tends to be larger than within-observer error (between-observer error range: 0.5–5%; Breuer et al. 2007; Barrickman et al. 2015; Berghänel et al. 2015; Galbany et al. 2016; Lu et al. 2016; Wright et al. 2019). Switching to an automated inter-laser distance measurement will reduce uncertainty due to between-observer error to the same proportion as for within-observer error, assuming the ratio of the two components of variation—inter-laser distance and inter-landmark distance—is similar for within-observer error and between-observer error. However, we expect that greater level of uncertainty in between-observer error comes from the inter-landmark measurement, in which case the reduction in uncertainty when using these methods would be smaller than for within-observer error. Additionally, using an automated inter-laser measurement would help reduce uncertainty due to other sources of human error, including between-image measurement error of the same animal, and differences between direct measurements and parallel-laser photogrammetry measurements of an animal (Galbany et al. 2016). In effect, by decreasing measurement uncertainty due to human error, our methods increase the researcher's ability to measure real differences in body size between individuals and within individuals over time.

Choosing the best method for your research

Although the two automated methods produce similar results, they take different approaches. Depending on dataset size, field environment, and coding ability, one of these methods will be more suitable than the other. We discuss the main advantages and disadvantages of each method to highlight conditions under which they may be most suitable.

The *ImageJ* method is user friendly and easy to implement without specific coding knowledge. Therefore, it is ideal for smaller or shorter-term datasets, especially those for which the time costs of setting up and refining the *skimage* method may outweigh the time saved processing the images. In addition, the *ImageJ* method parameters (e.g., crop size, laser color) can be tested and adjusted easily within the *ImageJ* user interface and then copied into the underlying code; in contrast, the *skimage* method requires changes to the code to adapt the parameters. Finally, the *ImageJ* method works equally well with different numbers of laser spots, or lasers spots in different orientations; the orientation check of the *skimage* methods relies on three laser spots and would need to be adapted for devices with fewer laser spots, or devices in which the laser spots are not in a right triangle or straight line.

On the other hand, the *skimage* method has a very high success rate without manual intervention; the *ImageJ* method, requires hand-cropping of approximately half (for baboon images) or nearly all (for gorilla images) of the images before processing successfully. Second, the *skimage* method was more successful at identifying the laser spots on a novel dataset; the *skimage* method identified the laser spots for 98/100 of the baboon images, while the *ImageJ* method only identified the laser spots for 88/100 gorilla images, even after hand-cropping. Third, the *skimage* method is highly customizable and able to accommodate a wide variety of image processing tasks. While *ImageJ* has many image processing functions, its user interface makes it more difficult to access some of the less-used functions. Ultimately, the *skimage* method is ideal for larger or longer-term datasets and images with green backgrounds—situations in which the benefit of a more customized and hands-off method outweighs the costs of set-up time and time to gain specific technical knowledge.

Machine learning represents a highly versatile and promising future direction for parallel-laser photogrammetry. For example, processing machine learning masked images with the *ImageJ* method increased the success rate of the *ImageJ* method before hand-cropping by 43% (increase from 74/200 to 96/200; measurements not shown). Another advantage to machine learning is that the algorithm can be coded to focus on aspects that are difficult to describe with image processing. For example, a researcher could train a machine learning algorithm to identify the pattern of reptile scales or a complex plumage pattern, allowing the researcher to reliably detect their study subject in images. In addition, we see promise in using machine learning to automate the inter-landmark distance measurements. Several studies have already published machine learning networks that track body landmarks across frames of videos, suggesting that this goal may soon be within reach (Mathis et al. 2018; Martınez 2019; Sanakoyeu et al. 2020). The next step in this process will be to adapt this technology to identify landmarks on singular images. This could then be integrated with our automated methods for measuring the inter-laser distance to fully automate the photogrammetry measurement process.

Best practices

We recommend several best practices for researchers implementing either of these methods in their study system. First, precision of the inter-laser distance will always be improved when the physical distance between the laser beams (inter-beam distance) is larger. In our dataset, the percent difference between manual and automated image measurements tended to be higher when the inter-beam distance was smaller (Appendix: Table A4). Second, when testing and optimizing either automated method, we recommend using a set of approximately 100 trial images, all taken with the same image resolution. Third, when setting up an automated method with this set of trial images, we recommend using percent difference instead of or in addition to raw pixel difference to assess how well the method works. This is because the trial images will be taken from different distances, and one pixel will convert to a different physical size depending on that distance. And finally, each new use of either of these methods will require validation. We recommend testing the automated method against manually-measured images in a similar fashion to the analyses presented here.

Conclusion

Interest in using parallel laser photogrammetry to measure the body size of wild animals has increased dramatically in the past decade. The method offers great potential for expanding our understanding of growth and body size differences within and between wild animal species and populations; this understanding, in turn, will inform

conservation practices as well as evolutionary and ecological theory. However, parallel laser photogrammetry is highly labor-intensive and researchers face challenges associated with the accuracy and precision of body size measurements. To achieve its full potential, parallel laser photogrammetry must be refined in efficiency, precision, and accuracy. The two methods presented here are a significant step forward in increasing efficiency and precision to provide high-throughput calibration that is accurate and precise, and we encourage future researchers to apply these methods to their study systems.

Appendix

Skimage method without machine learning

As noted in 'Schematics and Workflow for the *skimage* and *ImageJ* Methods', the *skimage* method can also be performed without the pre-processing step of machine learning to mask the gorilla.

Here we compare the results of the *skimage* method with machine learning (as presented in the manuscript, Table A1: row 1) to the s*kimage* method using only image processing steps on the full image, not using the machine learning masks, '*skimage* without machine learning' (Table A1: row 2). This was performed on the original dataset of 100 gorilla images. The image processing takes longer without the machine learning pre-processing step (Table A2). The *skimage* without machine learning method returned measurements for 100% of images; however, in one image the laser spots were mis-identified (not included in Table A1). Using *skimage* with and without machine learning produces very similar results on the gorilla dataset (Table A2). Thus, using the *skimage* method without machine learning may be more suitable for researchers without access to the processing power needed to run the machine learning step, or who are unfamiliar with machine-learning algorithms. However, the image processing code was developed for use with photos of dark animals against green backgrounds. Thus, for researchers who are using images that are distinctly different in color or animal species, implementing the machine learning step on their photographs will almost certainly yield better-quality masking than image processing approaches based on color alone.

Table A3 compares the three methods as in Table 1, but it reports the absolute differences instead of the percent differences. Table A4 compares the three methods as in Table 1, but it provides percent differences as a function of inter-beam distance.

Table A2 Computing time (minutes) required for *skimage*, *skimage* without machine learning, and *ImageJ* methods to process 100 images. For *ImageJ* images that need to be hand-cropped, this takes approximately 5 additional seconds per image of manual effort. Note the gorilla images have a longer processing time because they have more pixels per image

Dataset	*skimage* with machine learning (minutes)	*skimage* without machine learning (minutes)	*ImageJ (minutes)*
Baboon images	107	71	3.25
Gorilla images	204	190	5.25

Table A3 Absolute percent differences [and absolute pixel differences] among inter-laser distances measured manually vs. the *ImageJ* method, manually vs. the *skimage* method and via the *ImageJ* method vs. the *skimage* method on both study animal datasets; diff = difference

Species	Comparison	Mean |% diff| [|pixel diff|]	SD of |% diff| [|pixel diff|]
Gorilla	**Skimage vs. manual**	**0.483 [0.668]**	**0.518 [0.619]**
Gorilla	ImageJ vs. manual	0.693 [1.07]	0.954 [1.68]
Gorilla	Skimage vs. ImageJ	0.538 [0.817]	0.843 [1.47]
Baboon	**ImageJ vs. manual**	**0.515 [0.560]**	**0.740 [0.547]**
Baboon	Skimage vs. manual	0.595 [0.694]	0.681 [0.617]
Baboon	ImageJ vs. skimage	0.414 [0.424]	0.796 [0.518]

Table A1 Percent differences [pixel differences] among inter-laser distances measured manually vs. the *skimage* method with machine learning and manually vs. the *skimage* without machine learning method on the gorilla dataset; diff = difference

	Method	Successful images	Mean % diff [pixel diff]	SD % diff [pixel diff]	Range of % diff [pixel diff]
1	*skimage* with machine learning	100	– 0.004 [0.004]	0.710 [0.913]	– 1.58, 4.34 [– 2.88, 3.33]
2	*skimage* without machine learning	99	0.011 [0.037]	0.679 [0.904]	– 1.60, 3.73 [– 2.84, 3.57]

Table A4 Percent differences [pixel differences] as a function of inter-beam distance (cm); data are from rows 1 and 4 of Table 1, split by inter-beam distance in centimeters, diff = difference

	Species	Comparison	Inter-beam distance (cm)	# Images	Mean % diff [pixel diff]	SD of % diff [pixel diff]	Range of % diff [pixel diff]
1	Gorilla	Skimage vs. manual	2	19	0.153 [0.187]	1.23 [1.20]	– 1.48, 4.34 [– 1.63, 3.33]
2	Gorilla	Skimage vs. manual	4	76	– 0.034 [– 0.034]	0.523 [0.853]	– 1.58, 1.11 [– 2.88, 2.14]
3	Gorilla	Skimage vs. manual	4.5	5	– 0.169 [– 0.119]	0.628 [0.517]	– 1.03, 0.582 [– 0.628, 0.437]
4	Baboon	ImageJ vs. manual	2	8	1.20 [0.555]	1.78 [0.776]	– 0.519, 4.94 [– 0.226, 2.15]
5	Baboon	ImageJ vs. manual	4	92	– 0.096 [– 0.093]	0.712 [0.767]	– 3.98, 1.54 [– 3.18, 2.11]

Supplementary Information The online version contains supplementary material available at https://doi.org/10.1007/s42991-021-00174-7.

Acknowledgements This paper was a collaboration between researchers associated with the Bwindi Gorilla Research Project and the Amboseli Baboon Research Project. We thank the Uganda Wildlife Authority and the Uganda National Council for Science and Technology for permission to conduct research on mountain gorillas in Uganda and for support of this research. We are greatly indebted to the many field assistants who have contributed to this work, and to the Institute for Tropical Forest Conservation for providing logistical support. Particularly, we thank M. Akantorana, D. Musinguzi, J. Mutale, B. Turyananuka, for their long-term contributions to the Bwindi Gorilla Research Project. We also thank Edward Wright for help in the development and training needed for the data collection in Bwindi and Chen Zeng for expertise in developing the method. We thank Anna Lee for collecting baboon images, Elise Malone for measuring baboon images, and Emma Helmich for assisting with the development of the ImageJ method. Particular thanks go to the Amboseli Baboon Research Project directors (J. Altmann, S.C. Alberts, E.A. Archie, J. Tung), and the long-term field team (R.S. Mututua, S. Sayialel, J.K. Warutere, I.L. Siodi). For a complete set of acknowledgments of funding sources, logistical assistance, and data collection and management for the long-term baboon research, please visit http://amboselibaboons.nd.edu/acknowledgements/.

Author contributions Conceptualization: EJL, MER, and SCM; method development *skimage*: JLR, HY, MER, JG, AC, and SCM; method development *ImageJ*: EJL, RR, and EEM; data analysis: JLR and EJL; project administration: SCA, MMR, and SCM; writing—original draft: JLR and EJL; writing—review and editing**:** JLR, EJL, EEM, JG, MMR, SCA, MER, and SCM.

Funding The Bwindi Gorilla Research Project gratefully acknowledges the following funding support for this work: The Wenner-Gren Foundation (ICRG 123), National Science Foundation (NSF BCS 1753651), The George Washington University, The Max Planck Society, United States Fish and Wildlife Service Great Ape Fund and Berggorilla Regenwald Direkthlife. The Amboseli Baboon Research Project gratefully acknowledges the following specific support for this project: the National Science Foundation via a Graduate Research Fellowship to EJL (DGE1644868), the National Institute on Aging (R01AG053308), The Leakey Foundation, the Animal Behavior Society, the Society for the Study of Evolution, and Duke University.

Availability of data and material Data are available on Dryad data repository at https://doi.org/10.5061/dryad.51c59zw7d and on GitHub at http://github.com/ejlevy/Photogrammetry_Coding_InterLaser_Distance.

Code availability Code to run the automated methods are available at http://github.com/ejlevy/Photogrammetry_Coding_InterLaser_Distance.

Declarations

Conflict of interest The authors have no conflicts of interest to declare.

Ethics approval This research was approved by the IACUC at Duke University and adhered to all the laws and regulation governing research in Kenya and Uganda.

Consent to participate Not applicable.

Consent for publishing The authors gave consent to publish this paper.

References

Aleixo F, O'Callaghan SA, Ducla Soares L, Nunes P, Prieto R (2020) AragoJ: A free, open-source software to aid single camera photogrammetry studies. Methods Ecol Evol 11(5):670–677. https://doi.org/10.1111/2041-210X.13376

Altmann J, Alberts SC (2005) Growth rates in a wild primate population: ecological influences and maternal effects. Behav Ecol Sociobiol 57(5):490–501. https://doi.org/10.1007/s00265-004-0870-x

Barrickman NL, Schreier AL, Glander KE (2015) Testing parallel laser image scaling for remotely measuring body dimensions on mantled howling monkeys (*Alouatta palliata*). Am J Primatol 77(8):823–832. https://doi.org/10.1002/ajp.22416

Berger J (2012) Estimation of body-size traits by photogrammetry in large mammals to inform conservation. Conserv Biol 26(5):769–777. https://doi.org/10.1111/j.1523-1739.2012.01896.x

Bergeron P (2007) Parallel lasers for remote measurements of morphological traits. J Wildl Manag 71(1):289–292. https://doi.org/10.2193/2006-290

Berghänel A, Schülke O, Ostner J (2015) Locomotor play drives motor skill acquisition at the expense of growth: A life history trade-off. Sci Adv 1(7):e1500451. https://doi.org/10.1126/sciadv.1500451

Bevington P, Robinson DK (2002) Data reduction and error analysis for the physical sciences, 3rd edn. McGraw-Hill Education, New York City. https://doi.org/10.1063/1.4823194

Breuer T, Robbins MM, Boesch C (2007) Using photogrammetry and color scoring to assess sexual dimorphism in wild Western Gorillas (*Gorilla gorilla*). Am J Phys Anthropol 134(3):369–382. https://doi.org/10.1002/ajpa.20678

Clapham M, Miller E, Nguyen M, Darimont CT (2020) Automated facial recognition for wildlife that lack unique markings: a deep

learning approach for brown bears. Ecol Evol 10(23):12883–12892. https://doi.org/10.1002/ece3.6840

de Palmer Forest A (1912) The theory of measurements. McGraw-Hill Book Company, New York City. https://doi.org/10.1038/095342a0

Deakos MH (2010) Paired-laser photogrammetry as a simple and accurate system for measuring the body size of free-ranging manta rays *Manta alfredi*. Aquat Biol 10(1):1–10. https://doi.org/10.3354/ab00258

Durban JW, Parsons KM (2006) Laser-metrics of free-ranging killer whales. Mar Mamm Sci 22(3):735–743. https://doi.org/10.1111/j.1748-7692.2006.00068.x

Durban J, Fearnbach H, Burrows D, Ylitalo G, Pitman R (2017) Morphological and ecological evidence for two sympatric forms of Type B killer whale around the Antarctic Peninsula. Polar Biol 40(1):231–236. https://doi.org/10.1007/s00300-016-1942-x

Galbany J, Stoinski TS, Abavandimwe D, Breuer T, Rutkowski W, Batista NV, Ndagijimana F, McFarlin SC (2016) Validation of two independent photogrammetric techniques for determining body measurements of gorillas. Am J Primatol 78(4):418–431. https://doi.org/10.1002/ajp.22511

Galbany J, Abavandimwe D, Vakiener M, Eckardt W, Mudakikwa A, Ndagijimana F, Stoinski TS, McFarlin SC (2017) Body growth and life history in wild mountain gorillas (*Gorilla beringei beringei*) from Volcanoes National Park, Rwanda. Am J Phys Anthropol 163(3):570–590. https://doi.org/10.1002/ajpa.23232

Gardner JL, Peters A, Kearney MR, Joseph L, Heinsohn R (2011) Declining body size: a third universal response to warming? Trends Ecol Evol 26(6):285–291. https://doi.org/10.1016/j.tree.2011.03.005

Jeffreys G, Rowat D, Marshall H, Brooks K (2013) The development of robust morphometric indices from accurate and precise measurements of free-swimming whale sharks using laser photogrammetry. Marine Biological Association of the United Kingdom. J Mar Biol Assoc UK 93(2):309. https://doi.org/10.1017/S0025315412001312

Lourie HJ, Hoskins AJ, Arnould JP (2014) Big boys get big girls: Factors influencing pupping site and territory location in Australian fur seals. Mar Mamm Sci 30(2):544–561. https://doi.org/10.1111/mms.12056

Lu A, Bergman TJ, McCann C, Stinespring-Harris A, Beehner JC (2016) Growth trajectories in wild geladas (*Theropithecus gelada*). Am J Primatol 78(7):707–719. https://doi.org/10.1002/ajp.22535

Martınez GH (2019) OpenPose: whole-body pose estimation. Master's Thesis, Carnegie Mellon University

Mathis A, Mamidanna P, Cury KM, Abe T, Murthy VN, Mathis M, Bethge M (2018) DeepLabCut: markerless pose estimation of user-defined body parts with deep learning. Nat Neurosci 21(9):1281–1289. https://doi.org/10.1038/s41593-018-0209-y

Rohner C, Richardson A, Marshall A, Weeks S, Pierce S (2011) How large is the world's largest fish? Measuring whale sharks *Rhincodon typus* with laser photogrammetry. J Fish Biol 78(1):378–385. https://doi.org/10.1111/j.1095-8649.2010.02861.x

Rothman JM, Chapman CA, Twinomugisha D, Wasserman MD, Lambert JE, Goldberg TL (2008) Measuring physical traits of primates remotely: the use of parallel lasers. Am J Primatol 70(12):1191–1195. https://doi.org/10.1002/ajp.20611

Sanakoyeu A, Khalidov V, McCarthy MS, Vedaldi A, Neverova N (2020) Transferring dense pose to proximal animal classes. In: Proceedings of the IEEE/CVF Conference on computer vision and pattern recognition, pp 5233–5242. https://ieeexplore.ieee.org/xpl/conhome/1000147/all-proceedings

Schneider CA, Rasband WS, Eliceiri KW (2012) NIH Image to ImageJ: 25 years of image analysis. Nat Methods 9(7):671–675. https://doi.org/10.1038/nmeth.2089

Swenson JE, Adamič M, Huber D, Stokke S (2007) Brown bear body mass and growth in northern and southern Europe. Oecologia 153(1):37–47. https://doi.org/10.1007/s00442-007-0715-1

Tarugara A, Clegg BW, Gandiwa E, Muposhi VK, Wenham CM (2019) Measuring body dimensions of leopards (*Panthera pardus*) from camera trap photographs. PeerJ 7:e7630. https://doi.org/10.7717/peerj.7630

Vaid S, Cakan C, Bhandari M (2020) Using machine learning to estimate unobserved COVID-19 infections in North America. J Bone Jt Surg Am Vol. https://doi.org/10.2106/JBJS.20.00715

van der Walt S, Schönberger J, Nunez-Iglesias J, Boulogne F, Warner J, Yager N, Gouillart E, Yu T, the scikit-image contributors (2014) scikit-image: image processing in Python. PeerJ 2:e453. https://doi.org/10.7717/peerj.453

Webster T, Dawson S, Slooten E (2010) A simple laser photogrammetry technique for measuring Hector's dolphins (*Cephalorhynchus hectori*) in the field. Mar Mamm Sci 26(2):296–308. https://doi.org/10.1111/j.1748-7692.2009.00326.x

Weisgerber JN, Medill SA, McLoughlin PD (2015) Parallel-laser photogrammetry to estimate body size in free-ranging mammals. Wildl Soc B 39(2):422–428. https://doi.org/10.1002/wsb.541

Wijeyamohan S, Sivakumar V, Read B, Schmitt D, Krishnakumar S, Santiapillai C (2012) A simple technique to estimate linear body measurements of elephants. Curr Sci India 102(1):26–28

Wong JB, Auger-Méthé M (2018) Using laser photogrammetry to measure long-finned pilot whales (*Globicephala melas*). N S Inst Sci (NSIS) 49(2):269. https://doi.org/10.15273/pnsis.v49i2.8164

Wright E, Galbany J, McFarlin SC, Ndayishimiye E, Stoinski TS, Robbins MM (2019) Male body size, dominance rank and strategic use of aggression in a group-living mammal. Anim Behav 151:87–102. https://doi.org/10.1016/j.anbehav.2019.03.011

Wright E, Galbany J, McFarlin SC, Ndayishimiye E, Stoinski TS, Robbins MM (2020) Dominance rank but not body size influences female reproductive success in mountain gorillas. PLoS ONE 15(6):e0233235. https://doi.org/10.1371/journal.pone.0233235